PID controller design for disturbed multivariable systems

Y. Zhang, L.-S. Shieh and A.C. Dunn

Abstract: A linear-quadratic-regulator-based design methodology is proposed to design proportional-integral-derivative (PID) controllers for multivariable systems with load disturbances. Except for a few parameters that are preliminarily selected, most of the PID parameters are systematically tuned using the developed plant state-feedback and controller state-feedforward LQR approach, such that satisfactory performance with guaranteed closed-loop stability is achieved. In order to access the plant state variables and carry out disturbance rejection, an observer-based disturbance rejection technique is proposed, which through an 'equivalent disturbance' concept, retains the observation error to be used for disturbance compensation. This makes disturbance measurement unnecessary and the disturbance rejection tuning independent of the set-point response adjustment. A robust stability analysis is also included for the modelling error. An illustrative example is given for comparison with alternative techniques.

1 Introduction

The single-input single-output (SISO) proportional-integral-derivative (PID) controller is currently widely used in industry due to its simplicity in controller structure, robustness to constant disturbances, and the availability of numerous tuning methods. In principle, for any general plant, it is possible to design a PID controller using one of many available methods, depending on the required performance specifications. In practice, however, a few methods have become favoured due to their good approximation of process transfer functions produced from simplistic step response fitting, which enables them to work satisfactorily for certain processes. The two most widely accepted models that have emerged are the first-order plus dead time (FOPDT) and the second-order plus dead time (SOPDT) models. For high-order dynamical systems, PID parameter detuning [1–3] is sometimes necessary due to stability or system complexity. Fortunately, most real industrial processes can be accurately approximated by a FOPDT or SOPDT model, for which many effective design methods are available to design a PID controller. Hence, little effort is required to de-tune the PID parameters to meet the performance specifications of the original high-order systems.

PID controller design for multi-input multi-output (MIMO) systems is a much more complicated problem compared to the SISO case. Apart from the fact that MIMO PID controllers have many more parameters than SISO PID controllers, loop interaction (or coupling) is a more challenging problem. This makes it difficult for the designer to design each loop independently, as the tuning of controller variables of one loop will affect the performance of the others and may even destabilise the entire system. Whereas multivariable PID control has been researched extensively for over 30 years, with various design methodologies having been proposed [4–10], the task of developing a satisfactory design procedure for MIMO PID controllers remains a difficult problem [11]. For example, the controller design specifications such as the gain-phase margin, bandwidth, etc. [10], for MIMO systems are still not well defined. So, in many existing approaches for MIMO PID controller design, the plant is often assumed to be of, or can be decoupled into, a set of SISO systems. Then, the resulting decentralised (or diagonal) PID controller design for a MIMO system is analogous to the scalar PID controller design for the SISO system. However, if the coupling is significant, especially for the high-dimensional system, the decentralised PID controller may fail to give acceptable responses. In such cases, a centralised (or fully cross-coupled) PID controller is needed because it can inherently compensate for the coupling [6].

We now propose a feedback/feedforward design methodology, in which the PID tuning problem is transformed into a linear quadratic regulator (LQR) design through proper arrangement of the state space equation of the cascaded system. Most of the PID parameters are determined systematically through such a tuning process, except for a few parameters that are preselected. Compared with existing methods, our proposed method offers the following advantages: (i) MIMO PID controlled system stability is guaranteed during the tuning process; and (ii) there are no specific requirements on system stability, low-degree and/or low-dimension model, minimum-phase property and plant decoupling.

While the primary focus of the proposed PID LQR tuning method is on the set-point response of the closed-loop system, we recognise that a good set-point response does not necessarily guarantee acceptable disturbance rejection [12]. Therefore, in cases where load disturbances exist at the output points, we also propose a method for disturbance rejection. Feedforward control [13] may be used to eliminate/reduce the output disturbance directly, making the disturbance rejection tuning independent of the controller

IEE Proceedings online no. 20040751

doi: 10.1049/ip-cta:20040751

Paper first received 27th October 2003 and in revised form 18th May 2004. Originally published online 26th October 2004

The authors are with the Department of Electrical and Computer Engineering, University of Houston, Houston, TX 77204-4005, USA

design. However, this approach requires the disturbance to be measurable. Due to the existence of the biased load disturbance, the exact plant state is hard to estimate, and in some cases an integral observer has to be constructed [14]. Nevertheless, the resulting plant state is in general not very useful in attenuating the disturbance effects. Some authors use the extended state observer [15] or disturbance observer [16] to estimate the disturbances, and then make appropriate compensation. However, the resulting controller/observer structure is usually very complicated.

Recognising that the state estimation error in conjunction with output disturbance is difficult to remove, is it still possible for it to be used for disturbance compensation? This is the key point explored in the proposed observer-based disturbance rejection technique. Using only a conventional observer in the presence of load disturbance will inevitably result in some estimation error. In this case, the actual feedback control gain will be composed of two parts: (i) the exact plant state feedback as expected; and (ii) an additional feedback component that is introduced by the estimation errors. This additional feedback component can be used as feedforward compensation for the output disturbances, provided that the observer gain is properly selected. The residual disturbance after compensation will generate the so-called 'equivalent disturbances' that can be used as a performance index, for disturbance rejection in the process of observer gain adjustment. The advantages of such a method are obvious, as the disturbance rejection tuning is now independent of the state-feedback gain adjustment, while the controller/observer structure remains simple and does not require disturbance measurement.

2 Problem formulation

Consider a unity-output feedback MIMO analog plant $\boldsymbol{G}_1(s) \in R^{p1\times m1}$ in cascade with a MIMO analog PID controller $\boldsymbol{G}_2(s) \in R^{m1\times p1}$. Also, suppose output disturbance $\boldsymbol{d}(t) \in R^{p1}$ exists at the output point as shown in Fig. 1.

Let the minimal realisation of the analog plant $\boldsymbol{G}_1(s)$ be:

$$\dot{\boldsymbol{x}}_1(t) = \boldsymbol{A}_1\boldsymbol{x}_1(t) + \boldsymbol{B}_1\boldsymbol{u}_1(t) \quad \boldsymbol{x}_1(0) = \boldsymbol{x}_{10} \tag{1a}$$

$$\boldsymbol{y}_1(t) = \boldsymbol{C}_1\boldsymbol{x}_1(t) \tag{1b}$$

where $\boldsymbol{x}_1(t) \in R^{n1}, \boldsymbol{u}_1(t) \in R^{m1}, \boldsymbol{y}_1(t) \in R^{p1}$, and $\boldsymbol{A}_1, \boldsymbol{B}_1, \boldsymbol{C}_1$ are constant matrices of appropriate dimensions. Let the entire system output be the sum of the plant output and load disturbance:

$$\boldsymbol{y}(t) = \boldsymbol{y}_1(t) + \boldsymbol{d}(t) \tag{2}$$

where $\boldsymbol{y}(t) \in R^{p1}$, $\boldsymbol{d}(t) \in R^{p1}$. Each component of the MIMO PID controller $\boldsymbol{G}_2(s) \in R^{m1\times p1}$ is described as:

$$G_{2ij}(s) = K_{\mathrm{P}ij} + \frac{K_{\mathrm{I}ij}}{s} + \frac{K_{\mathrm{D}ij}s}{s+\alpha_{ij}} \tag{3}$$

for $i = 1, 2, \ldots, m1$ and $j = 1, 2, \ldots, p1$. Parameters of the PID controller, $K_{\mathrm{P}ij}$, $K_{\mathrm{I}ij}$, $K_{\mathrm{D}ij}$, and filter factor α_{ij} are constants to be determined.

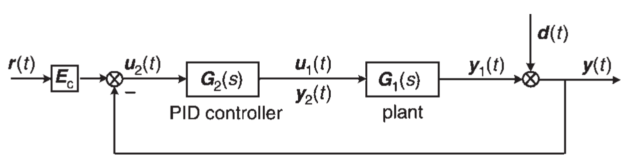

Fig. 1 *Continuous-time cascaded system*

The filter factor α for the derivative term can be chosen by design specifications [17]. Based on the internal model principle (IMP) [13], steady-state disturbance compensation requires that the disturbance generating polynomial be included as part of the controller denominator. Thus, we can determine denominators of the controller through setting the filter factors (i.e. $s + \alpha_{ij}$ in (3)) as those of the load disturbance denominators. When the load disturbance is different for each subsystem, we can adjust the filter factors accordingly. Then, the transfer function matrix of the controller can be rewritten from (3) as follows:

$$\boldsymbol{G}_2(s) = \frac{\boldsymbol{E}_1 s^{p1+1} + \boldsymbol{E}_2 s^{p1} + \ldots + \boldsymbol{E}_{\mathrm{p}1+1}s + \boldsymbol{E}_{\mathrm{p}1+2}}{s\prod_{j=1}^{p1}(s+\alpha_j)} \tag{4}$$

where parameter matrices $\boldsymbol{E}_1$, $\boldsymbol{E}_2 \ldots \boldsymbol{E}_{p1+2}$ are unknowns to be determined.

Remark 1: It should be noted that when the poles of a high-degree asymptotically stable disturbance model are known, the first-degree filter in (4) can be approximately determined via model reduction methods [18, 19], or we can use the smallest pole as the filter factors. The designed PID controller can eliminate the steady-state disturbance and control errors. However, it is unable to completely eliminate the steady-state disturbance errors if the load disturbance is a sinusoidal disturbance.

Although our proposed methodology for MIMO PID controller design does not require that the plant be of, or can be decoupled into a form of, SISO systems, we let the plant be diagonally dominant, so that the designed controller would be near to being decentralised. The static decoupler [13, 20] is widely used as a precompensator in MIMO system design for achieving approximate decoupling. In general, this decoupler is defined as $\boldsymbol{D}_2 = \boldsymbol{G}_1^{-1}(0)$, where $\boldsymbol{G}_1(0)$ is non-singular. We can make the plant statically decoupled by setting $\boldsymbol{E}_1 = \boldsymbol{D}_2 = \boldsymbol{G}_1^{-1}(0)$ in (4), which then gives:

$$\boldsymbol{G}_2(s) = \boldsymbol{D}_2 + \frac{\boldsymbol{F}_2 s^{p1} + \boldsymbol{F}_3 s^{p1-1} + \cdots + \boldsymbol{F}_{\mathrm{p}1+1}s + \boldsymbol{F}_{\mathrm{p}1+2}}{s\prod_{j=1}^{p1}(s+\alpha_j)} \tag{5a}$$

where $\boldsymbol{F}_2$, $\boldsymbol{F}_3, \ldots, \boldsymbol{F}_{p1+2}$ are constant matrices to be determined.

For simplicity, we can first select the MIMO PID controller as:

$$\boldsymbol{G}_2(s) = \boldsymbol{D}_2 + \mathrm{diag}\left(\frac{1}{s(s+\alpha_j)}\right) \quad \text{for } j = 1, 2, \ldots, p1 \tag{5b}$$

and leave further parameter adjustment to the next tuning phase.

Then, the minimal realisation of the preliminarily designed cascaded PID controller $\boldsymbol{G}_2(s)$ can be written as:

$$\dot{\boldsymbol{x}}_2(t) = \boldsymbol{A}_2\boldsymbol{x}_2(t) + \boldsymbol{B}_2\boldsymbol{u}_2(t) \quad \boldsymbol{x}_2(0) = 0 \tag{6a}$$

$$\boldsymbol{y}_2(t) = \boldsymbol{C}_2\boldsymbol{x}_2(t) + \boldsymbol{D}_2\boldsymbol{u}_2(t) = \boldsymbol{u}_1(t) \tag{6b}$$

$$\boldsymbol{u}_2(t) = -\boldsymbol{y}(t) + \boldsymbol{E}_c\boldsymbol{r}(t) \tag{6c}$$

where $\boldsymbol{x}_2(t) \in R^{n2}, \boldsymbol{u}_2(t) \in R^{p1}, \boldsymbol{y}_2(t) \in R^{m1}, \boldsymbol{r}(t) \in R^{p1}$, and $\boldsymbol{A}_2, \boldsymbol{B}_2, \boldsymbol{C}_2, \boldsymbol{D}_2, \boldsymbol{E}_\mathrm{c}$ are constant matrices of appropriate dimensions.

3 The MIMO PID controller tuning with state-feedback and state-feedforward LQR

Initially, consider a disturbance-free system with a pre-designed analog PID controller. Based on such a predesigned controller, further tuning is necessary to achieve satisfactory closed-loop performance. The basic idea of our methodology is to transform the PID tuning problem to that of optimal design. To achieve this aim, we formulate the closed-loop cascaded systems in Fig. 1 into an augmented system as:

$$\dot{\boldsymbol{x}}_e(t) = \boldsymbol{A}_e\boldsymbol{x}_e(t) + \boldsymbol{B}_e\boldsymbol{u}_1(t) + \mathbf{E}_e\mathbf{r}(t)$$
$$\boldsymbol{y}_e(t) = \boldsymbol{y}_1(t) = \boldsymbol{C}_e\boldsymbol{x}_e(t) \qquad (7)$$

where

$$\boldsymbol{A}_e = \begin{bmatrix} \boldsymbol{A}_1 & \boldsymbol{0} \\ -\boldsymbol{B}_2\boldsymbol{C}_1 & \boldsymbol{A}_2 \end{bmatrix} \quad \boldsymbol{B}_e = \begin{bmatrix} \boldsymbol{B}_1 \\ \boldsymbol{0} \end{bmatrix} \quad \boldsymbol{E}_e = \begin{bmatrix} \boldsymbol{0} \\ \boldsymbol{B}_2\boldsymbol{E}_c \end{bmatrix}$$
$$\boldsymbol{x}_e = \begin{bmatrix} \boldsymbol{x}_1(t) \\ \boldsymbol{x}_2(t) \end{bmatrix} \quad \boldsymbol{C}_e = [\boldsymbol{C}_1 \quad \boldsymbol{0}]$$

and

$$\boldsymbol{u}_1(t) = -\boldsymbol{K}_1\boldsymbol{x}_1(t) - \boldsymbol{K}_2\boldsymbol{x}_2(t) - \boldsymbol{D}_2\boldsymbol{u}_2(t) \qquad (8)$$

where the state-feedback control gains $\boldsymbol{K}_1$ and $\boldsymbol{K}_2$ are to be designed in the following. For the convenience of LQR design of $\boldsymbol{u}_1(t)$, given the existence of the feedforward input term $\boldsymbol{D}_2\boldsymbol{u}_2(t)$ in (8), an alternative representation of the augmented system (7) can be described as:

$$\dot{\boldsymbol{x}}_e(t) = \hat{\boldsymbol{A}}_e\boldsymbol{x}_e(t) + \boldsymbol{B}_e\hat{\boldsymbol{u}}_1(t) + \hat{\boldsymbol{E}}_e\boldsymbol{r}(t) \qquad (9a)$$

$$\boldsymbol{y}_1(t) = \boldsymbol{y}_e(t) = \boldsymbol{C}_e\boldsymbol{x}_e(t) \qquad (9b)$$

where

$$\hat{\boldsymbol{u}}_1(t) = \boldsymbol{u}_1(t) + \boldsymbol{D}_2\boldsymbol{u}_2(t) \qquad (9c)$$

$$\boldsymbol{u}_2(t) = -\boldsymbol{y}_1(t) + \boldsymbol{E}_c\boldsymbol{r}(t) \qquad (9d)$$

and

$$\hat{\boldsymbol{A}}_e = \begin{bmatrix} \boldsymbol{A}_1 + \boldsymbol{B}_1\boldsymbol{D}_2\boldsymbol{C}_1 & \boldsymbol{0} \\ -\boldsymbol{B}_2\boldsymbol{C}_1 & \boldsymbol{A}_2 \end{bmatrix} \boldsymbol{B}_e = \begin{bmatrix} \boldsymbol{B}_1 \\ \boldsymbol{0} \end{bmatrix}$$
$$\hat{\boldsymbol{E}}_e = \begin{bmatrix} -\boldsymbol{B}_1\boldsymbol{D}_2\boldsymbol{E}_c \\ \boldsymbol{B}_2\boldsymbol{E}_c \end{bmatrix} \boldsymbol{x}_e = \begin{bmatrix} \boldsymbol{x}_1(t) \\ \boldsymbol{x}_2(t) \end{bmatrix} \boldsymbol{C}_e = [\boldsymbol{C}_1 \quad \boldsymbol{0}]$$

The state-feedback LQR for the augmented system (9) can be chosen as:

$$\hat{\boldsymbol{u}}_1(t) = -\boldsymbol{K}_e\boldsymbol{x}_e(t) \qquad (10)$$

where $\boldsymbol{K}_e = [\boldsymbol{K}_1, \boldsymbol{K}_2]$ with $\boldsymbol{K}_1 \in R^{m1\times n1}$ and $\boldsymbol{K}_2 \in R^{m1\times n2}$.

Let the quadratic cost function for the system (9) be:

$$\boldsymbol{J} = \int_0^\infty [\boldsymbol{x}_e^T(t)\boldsymbol{Q}\boldsymbol{x}_e(t) + \hat{\boldsymbol{u}}_1^T(t)\boldsymbol{R}\hat{\boldsymbol{u}}_1(t)dt \qquad (11)$$

where $\boldsymbol{Q} \geq 0$, $\boldsymbol{R} > 0$, $(\hat{\boldsymbol{A}}_e, \boldsymbol{B}_e)$ controllable and $(\hat{\boldsymbol{A}}_e, \boldsymbol{Q})$ observable. The optimal state-feedback control gain $\boldsymbol{K}_e$ in (10) that minimises the performance index (11) is given by:

$$\boldsymbol{K}_e = \boldsymbol{R}^{-1}\boldsymbol{B}_e^T\boldsymbol{P} \qquad (12a)$$

in which the matrix $\boldsymbol{P} > 0$ is the solution of the Riccati equation [21]:

$$\boldsymbol{P}\hat{\boldsymbol{A}}_e + \hat{\boldsymbol{A}}_e^T\boldsymbol{P} - \boldsymbol{P}\boldsymbol{B}_e\boldsymbol{R}^{-1}\boldsymbol{B}_e^T\boldsymbol{P} + \boldsymbol{Q} = \boldsymbol{0} \qquad (12b)$$

The resulting closed-loop system becomes:

$$\dot{\boldsymbol{x}}_e(t) = (\hat{\boldsymbol{A}}_e - \boldsymbol{B}_e\boldsymbol{K}_e)\boldsymbol{x}_e(t) + \hat{\boldsymbol{E}}_e\boldsymbol{r}(t) \qquad (13)$$

which is asymptotically stable due to the property of LQR design.

Remark 2: Note that the closed-loop performance of the LQR-based design depends on the specification of the weighting matrices $\boldsymbol{Q}$ and $\boldsymbol{R}$ in (11). In order to achieve a specific performance, sometimes a trial-and-error process is needed for selection of the weighting matrices. This becomes increasingly more difficult, however, with the increase in system dimension. Alternatively, there are some other systematical ways in selecting the weighting matrices such as regional pole assignment [22–25].

Lemma 1 [24]*:* Let $(\hat{\boldsymbol{A}}_e, \boldsymbol{B}_e)$ be the pair of the given open-loop system in (9) and $h > 0$ represents the prescribed degree of relative stability. Then the closed-loop system $\hat{\boldsymbol{A}}_e - \boldsymbol{B}_e\boldsymbol{R}^{-1}\boldsymbol{B}_e^T\boldsymbol{P}$ has all its eigenvalues lying in the left of the $-h$ vertical line in the complex s-plane, where the matrix $\boldsymbol{P}$ is the solution of the following Riccati equation:

$$\boldsymbol{P}(\hat{\boldsymbol{A}}_e + h\boldsymbol{I}) + (\hat{\boldsymbol{A}}_e + h\boldsymbol{I})^T\boldsymbol{P} - \boldsymbol{P}\boldsymbol{B}_e\boldsymbol{R}^{-1}\boldsymbol{B}_e^T\boldsymbol{P} = \boldsymbol{0} \qquad (14)$$

where the matrix $\boldsymbol{I}$ is an $n \times n$ identity matrix and $\boldsymbol{R} > 0$.

In the illustrative example shown later, we also utilise the approach introduced in lemma 1 to carry out the regional pole assignment. This considerably simplifies the weighting matrices selection by assigning the weighting matrix $\boldsymbol{R} = \boldsymbol{I}$ and adjusting the single variable h.

Defining $\boldsymbol{K}_1$ as the plant state feedback gain, $\boldsymbol{K}_2$ as the controller feedforward gain in (10), then the desired state-feedback and state-feedforward control law $\boldsymbol{u}_1(t)$ in (8) can be indirectly determined from the state-feedback control law (10) and the relationships shown in (9c) and (9d) as:

$$\begin{aligned} \boldsymbol{u}_1(t) &= -\boldsymbol{K}_e\boldsymbol{x}_e(t) - \boldsymbol{D}_2\boldsymbol{u}_2(t) \\ &= -\hat{\boldsymbol{K}}_1\boldsymbol{x}_1(t) - \boldsymbol{K}_2\boldsymbol{x}_2(t) + \hat{\boldsymbol{E}}_c\boldsymbol{r}(t) \\ &= -\hat{\boldsymbol{K}}_e\boldsymbol{x}_e(t) + \hat{\boldsymbol{E}}_c\boldsymbol{r}(t) \end{aligned} \qquad (15)$$

where $\hat{\boldsymbol{K}}_1 = \boldsymbol{K}_1 - \boldsymbol{D}_2\boldsymbol{C}_1$, $\hat{\boldsymbol{K}}_e = \lfloor \hat{\boldsymbol{K}}_1, \ \boldsymbol{K}_2 \rfloor$ and $\hat{\boldsymbol{E}}_c = -\boldsymbol{D}_2\boldsymbol{E}_c$. Substituting the control law in (15) into (7), the designed closed-loop system becomes:

$$\begin{bmatrix} \dot{\boldsymbol{x}}_1(t) \\ \dot{\boldsymbol{x}}_2(t) \end{bmatrix} = \begin{bmatrix} \boldsymbol{A}_1 - \boldsymbol{B}_1(\boldsymbol{K}_1 - \boldsymbol{D}_2\boldsymbol{C}_1) & -\boldsymbol{B}_1\boldsymbol{K}_2 \\ -\boldsymbol{B}_2\boldsymbol{C}_1 & \boldsymbol{A}_2 \end{bmatrix} \begin{bmatrix} \boldsymbol{x}_1(t) \\ \boldsymbol{x}_2(t) \end{bmatrix} + \begin{bmatrix} -\boldsymbol{B}_1\boldsymbol{D}_2\boldsymbol{E}_c \\ \boldsymbol{B}_2\boldsymbol{E}_c \end{bmatrix} \boldsymbol{r}(t) \qquad (16a)$$

$$\boldsymbol{y}_1(t) = \boldsymbol{C}_1\boldsymbol{x}_1(t) \qquad (16b)$$

The block diagram of the designed augmented system (7) with the controller (15) is shown in Fig. 2.

The closed-loop stability of the PID controlled system is guaranteed due to the property of the LQR design. For the plant, its state space model is changed from $(\boldsymbol{A}_1, \boldsymbol{B}_1, \boldsymbol{C}_1)$ to $(\boldsymbol{A}_1 - \boldsymbol{B}_1\boldsymbol{K}_1, \boldsymbol{B}_1, \boldsymbol{C}_1)$, indicating that the poles of the plant are optimally relocated. As for the PID controller, its state space representation is tuned from $(\boldsymbol{A}_2, \boldsymbol{B}_2, \boldsymbol{C}_2, \boldsymbol{D}_2)$ to $(\boldsymbol{A}_2, \boldsymbol{B}_2, \boldsymbol{K}_2, \boldsymbol{D}_2)$, which means that all transmission zeros of the PID controller are optimally adjusted. Compared with existing methods, the advantages of our method are: (i) the MIMO PID parameters are systematically tuned with respect to both plant and controller, while the closed-loop

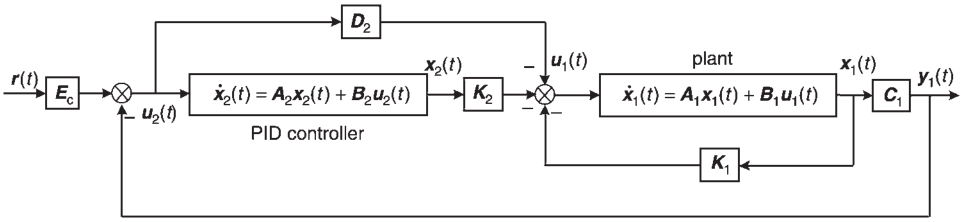

Fig. 2 *PID controlled system*

system stability is guaranteed; and (ii) there are no specific requirements on system stability, low-degree and/or low-dimension model, minimum-phase property and plant decoupling.

4 Observer-based disturbance rejection

So far, only steady-state disturbance compensation based on IMP has been considered, through setting the filter factor of the PID controller as that of the load disturbance denominator in the preliminary design phase. For our proposed disturbance rejection method, a multi-objective observer is used for both state estimation and disturbance rejection. The idea is to retain the observation error, which when properly adjusted provides feedforward compensation for the output disturbance. Thus, disturbance rejection can be achieved through the simple structure of a conventional observer.

For simplicity, we assume that both the plant and the observer have zero initial conditions. The initial condition error, which is regarded as part of the output disturbance, is discussed later. Suppose that the state space model of the plant $G_1(s)$ is:

$$\dot{x}_1(t) = A_1x_1(t) + B_1u_1(t) \tag{17a}$$

$$y_1(t) = C_1x_1(t) \tag{17b}$$

with the entire system output being the sum of the plant output and load disturbance as:

$$y(t) = y_1(t) + d(t) \tag{18}$$

We then design an observer, whose dynamic function is the same as that of the plant:

$$\dot{\hat{x}}_1(t) = A_1\hat{x}_1(t) + B_1u_1(t) - J_o[C_1\hat{x}_1(t) - y(t)] \tag{19}$$

in which $\hat{x}_1(t)$ represents the observed state, corresponding to the real state $x_1(t)$.

Then we have:

$$\dot{\hat{x}}_1(t) = A_1\hat{x}_1(t) + B_1u_1(t) - J_o[C_1\hat{x}_1(t) - C_1x_1(t) - d(t)] \tag{20}$$

with the observation error defined as:

$$e(t) = \hat{x}_1(t) - x_1(t) \tag{21}$$

Subtracting (17*a*) from (20), we get the observation error dynamic function as:

$$\dot{e}(t) = (A_1 - J_oC_1)e(t) + J_od(t) \tag{22}$$

Taking the Laplace transform of both sides, we get:

$$e(s) = [sI - (A_1 - J_oC_1)]^{-1}J_o \cdot d(s) \tag{23}$$

From (22), we find that a high observer gain J_o is needed in order to quickly remove the observation error; while on the other hand, high J_o will also amplify the disturbance. According to the existing observer design theory [21], a compromise has to be made between speedy response and sensitivity to disturbances and noise. However, this view is incomplete in one important aspect; it neglects the plant state-feedback dynamics. In fact, a high gain observer does not necessarily amplify the output deviation caused by disturbance, but may even provide some compensation for it.

From (20), we find that the observation error will inevitably exist due to output disturbance, and that the observed state feedback can be regarded as:

$$K_1\hat{x}_1(t) = K_1x_1(t) + K_1e(t) \tag{24}$$

where, the first term $K_1x_1(t)$ in the right-hand side of (24) is the exact plant state feedback as in the previous derivation, while the other term $K_1e(t)$ comes from the observation error. The configuration is shown in Fig. 3.

From (23), we get:

$$K_1e(s) = K_1[sI - (A_1 - J_oC_1)]^{-1}J_o \cdot d(s) \tag{25}$$

from which we can further separate $K_1e(t)$ from $K_1x_1(t)$ as shown in Fig. 4.

The observation error feedback can then be isolated from the exact state feedback, as shown in Fig. 5, in which $G_P(s) = C_1[sI - (A_1 - B_1K_1)]^{-1}B_1$, $\hat{G}_o(s) = K_1[sI - (A_1 - J_oC_1)]^{-1}J_o$, and $G_c(s) = -[K_2(sI - A_2)^{-1}B_2 + D_2]$.

We find that this additional feedback component, which comes from the feedback of the observation error, actually acts as feedforward control for the output disturbance.

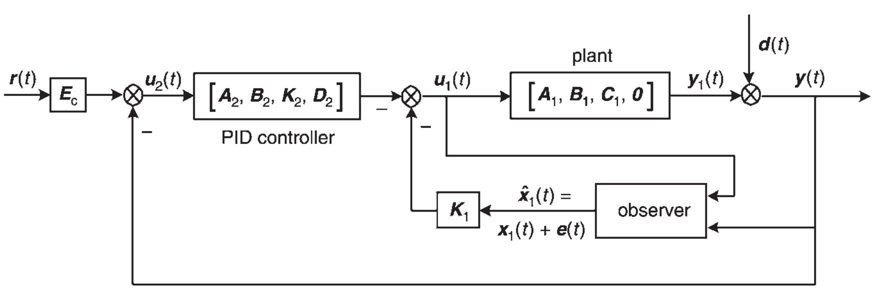

Fig. 3 *Observer structure*

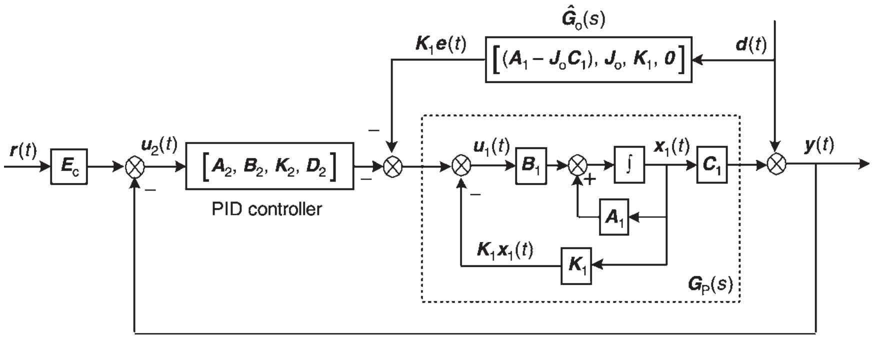

Fig. 4 *Observation error separation*

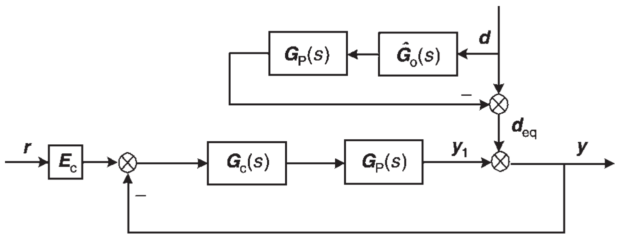

Fig. 5 *'Equivalent disturbance' structure*

The residual disturbance after feedforward compensation generates the so-called 'equivalent disturbance' as:

$$d_{eq}(s) = [I - G_P(s)\hat{G}_o(s)] \cdot d(s) \tag{26}$$

When the observer gain J_o is properly selected, the 'equivalent disturbance' will be close to zero. Note that it is almost impossible to reach complete compensation, because $G_P(s)\hat{G}_o(s)$ is only partially controllable only through the observer gain J_o, and the final output value of $G_P(s)\hat{G}_o(s)$ cannot be precisely adjusted through a weighting matrix due to its being unrealisable at the disturbance input point. Nonetheless, this partial compensation considerably attenuates the disturbance effects.

The proposed 'equivalent disturbance' concept provides an interesting viewpoint to evaluate the state observation error. It can be applied in the adjustment of the observer gain J_o, so that the resulting system would have less output deviation caused by output disturbance. The advantage of such a method is obvious, as the disturbance rejection tuning is independent of the state-feedback gains, and disturbances do not need to be measurable. Also, no extra components are needed to implement the proposed feedforward compensation.

Next, we investigate the effect of initial conditions. Suppose the state space model of the plant $G_1(s)$ described in (17) has initial condition $x_1(0)$, with the designed observer having zero initial conditions. Taking the Laplace transform of both sides and simplifying we get:

$$y_1(s) = [C_1(sI - A_1)^{-1}B_1]u(s) + C_1(sI - A_1)^{-1}x_1(0) \tag{27}$$

with corresponding time-domain solution as:

$$y_1(t) = C_1x_1(t) + y_\Delta(t) \tag{28}$$

where $y_\Delta(t) = L^{-1}[C_1(sI - A_1)^{-1}x_1(0)]$.

Then, the overall system output is obtained from (18) as:

$$y(t) = C_1x_1(t) + \bar{d}(t) \tag{29}$$

in which, $\bar{d}(t) = y_\Delta(t) + d(t)$. This means the output deviation caused by the initial condition error can be regarded as part of the output disturbance. So, the designed system based on the 'equivalent disturbance' concept is also less influenced by the initial condition error.

5 Robust stability analysis

There always exists some mismatch between the mathematical plant model and the real physical system, which is called the modelling error. The modelling error may arise from the time-delay rational approximation, non-linear system linearity, and parameter uncertainty, etc. Some robustness analysis is needed if the modelling error cannot be ignored. The additive modelling error is defined as the difference between the true plant model and the nominal plant model:

$$\Delta G_1(s) = \hat{G}_1(s) - G_1(s) \tag{30}$$

Correspondingly, there will exist an additional output term due to the modelling error:

$$\Delta y_1(s) = \Delta G_1(s) \cdot u(s) \tag{31}$$

Next, we analyse the robust stability in the case of modelling errors (Fig. 6). Since the external output disturbance has no effect on the stability analysis, we assume there is no external disturbance in the following.

Similar to the output disturbance consequence in (22), the additional output term due to modelling error will also lead to a similar observation error of:

$$\dot{e}(t) = (A_1 - J_oC_1)e(t) + J_o\Delta y_1(t) \tag{32}$$

with the corresponding Laplace transfer function of:

$$e(s) = [sI - (A_1 - J_oC_1)]^{-1}J_o \cdot \Delta y_1(s) \tag{33}$$

Then, the observed state feedback can be regarded as:

$$K_1\hat{x}_1(t) = K_1x_1(t) + K_1e(t) \tag{34}$$

where the first term $K_1x_1(t)$ on the right-hand side of (34) is the exact state feedback of the nominal plant as previously derived, with the second term $K_1e(t)$ from the observation error due to modelling error. From (33), we get:

$$K_1e(s) = K_1[sI - (A_1 - J_oC_1)]^{-1}J_o \cdot \Delta y_1(s) \tag{35}$$

Thus, we can further separate the observation error as shown in Fig. 7.

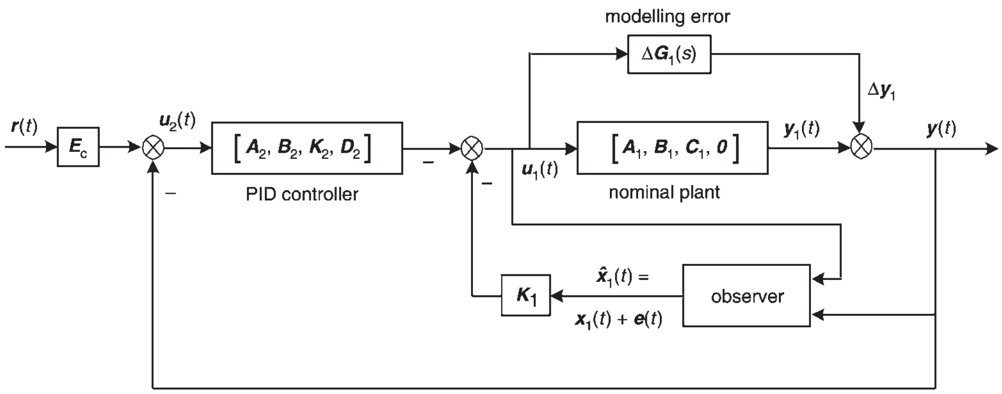

Fig. 6 *Observation error due to modelling error*

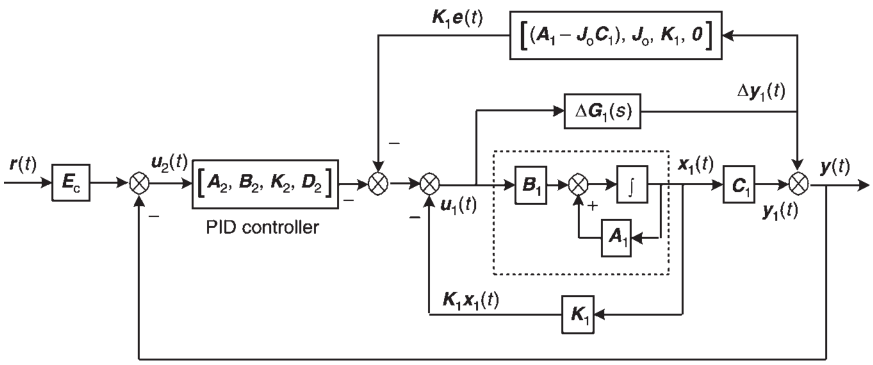

Fig. 7 *Observation error (due to the modelling error) separation*

Define $G_A(s)=(sI-A_1)^{-1}B_1$, $G_c(s)=-[K_2(sI-A_2)^{-1}B_2+D_2]$, $G_K(s)=K_1(sI-A_1)^{-1}B_1$, and $\hat{G}_o(s)=K_1[sI-(A_1-J_oC_1)]^{-1}J_o$.

Obviously, $G_1(s)=C_1(sI-A_1)^{-1}B_1=C_1G_A(s)$.

Assuming the upper bound $\bar{l}(s)$ of the additive modelling error as:

$$\Delta G_1(s)=\bar{l}(s)\cdot\Delta \tag{36}$$

where Δ is the normalised perturbation, that is, $\|\Delta\|_\infty=1$, then we get the configuration shown in Fig. 8.

It follows from robust stability analysis [26] that the system in Fig. 8 is asymptotically stable if:

$$\|T_{ab}(s)\|_\infty=\Big\|\bar{l}(s)\cdot G_x(s)\cdot\hat{G}_o(s)\cdot S(s)\cdot\Big[\hat{G}_o^{-1}(s)G_c(s),I\Big]\Big\|_\infty<I, \tag{37}$$

where $S(s)$ is the sensitivity function of the closed-loop system, i.e. $S(s)=[I+G_c(s)G_P(s)]^{-1}$, $G_P(s)$ is the state-feedback controlled nominal plant, i.e. $G_P(s)=C_1[sI-(A_1-B_1K_1)]^{-1}B_1=G_1(s)G_x(s)$, and $G_x(s)=[I+G_K(s)]^{-1}$. Through the above analysis, we find that the system is still robustly stable in case of modelling error, as long as condition (37) is satisfied.

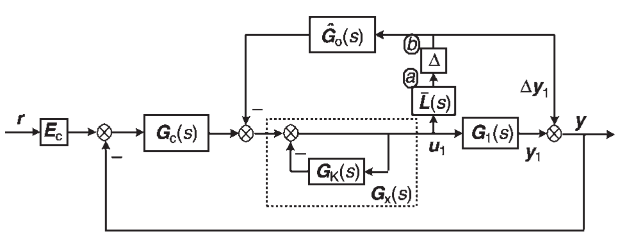

Fig. 8 *Modelling error structure for robust analysis*

6 An illustrative example

Consider a model of an industrial-scale polymerisation reactor [20]:

$$\begin{bmatrix} y_1(s) \\ y_2(s) \end{bmatrix}=\begin{bmatrix} \dfrac{22.89e^{-0.2s}}{4.572s+1} & \dfrac{-11.64e^{-0.4s}}{1.807s+1} \\ \dfrac{4.689e^{-0.2s}}{2.174s+1} & \dfrac{5.80e^{-0.4s}}{1.801s+1} \end{bmatrix}\begin{bmatrix} u_1(s) \\ u_2(s) \end{bmatrix}+\begin{bmatrix} \dfrac{-4.243e^{-0.4s}}{3.445s+1} \\ \dfrac{-0.601e^{-0.4s}}{1.982s+1} \end{bmatrix}d(s) \tag{38}$$

where $y_1(s)$ and $y_2(s)$ are two measurements representing the reactor condition, $u_1(s)$ and $u_2(s)$ are the set-points of two reactor feed-flow loops and disturbance $d(s)$ is the purge flow rate of the reactor. Due to the existence of the small dead time compared with the dominant time constant [27], a first-order Pade approximation model [28] is introduced as:

$$e^{-sT}\approx\frac{2-sT}{2+sT} \tag{39}$$

It is noted that if the dead time is relatively large compared with the dominant time constants, a high-order Pade approximation model is suggested.

Substituting (39) into (38), we get the parameter matrices of the minimal realisation of nominal plant $G_1(s)$ as:

$$A_1 = \begin{bmatrix} -10 & 0 & 0 & 0 & 0 & 0 \\ 0 & -5 & 0 & 0 & 0 & 0 \\ 0 & 0 & -0.5552 & 0 & 0 & 0 \\ 0 & 0 & 0 & -0.5534 & 0 & 0 \\ 0 & 0 & 0 & 0 & -0.4600 & 0 \\ 0 & 0 & 0 & 0 & 0 & -0.2187 \end{bmatrix}$$

$$B_1 = \begin{bmatrix} 1 & 0 \\ 0 & 1 \\ 0 & 1 \\ 0 & 1 \\ 1 & 0 \\ 1 & 0 \end{bmatrix}$$

$$C_1 = \begin{bmatrix} -10.2370 & 14.4866 & 0 & -8.0450 & 0 & 5.2304 \\ -4.5217 & -7.2454 & 4.0250 & 0 & 2.3649 & 0 \end{bmatrix} \tag{40}$$

The initial design for the PID controller $G_2(s)$ can be carried out as (5b) of Section 2 to get:

$$G_2(s) = D_2 + \mathrm{diag}\left\{\frac{1}{s(s+\alpha_j)}\right\} \quad \text{for } j = 1, 2, \ldots, p1 \tag{41a}$$

where D_2 is selected as the static decoupler, i.e. $D_2 = G_1^{-1}(0)$. The filter factor α_j can be chosen as the load disturbance denominator for steady-state disturbance compensation according to IMP. Particularly note that the time-delay term in the load disturbance is not necessarily considered in the PID controller design, because it makes no difference for the closed-loop performance if a load disturbance enters directly at the plant output or after passing through a time delay [29]. The preliminarily designed PID controller $G_2(s)$ is given as:

$$G_2(s) = \begin{bmatrix} 0.0310 & 0.0621 \\ -0.0250 & 0.1222 \end{bmatrix} + \begin{bmatrix} \frac{1}{s(s+0.2903)} & 0 \\ 0 & \frac{1}{s(s+0.5045)} \end{bmatrix} \tag{41b}$$

with its corresponding minimal realisation as:

$$A_2 = \begin{bmatrix} 0 & 0 & 0 & 0 \\ 0 & 0 & 0 & 0 \\ 0 & 0 & -0.2903 & 0 \\ 0 & 0 & 0 & -0.5045 \end{bmatrix} \quad B_2 = \begin{bmatrix} 1 & 0 \\ 0 & 1 \\ 1 & 0 \\ 0 & 1 \end{bmatrix}$$

$$C_2 = \begin{bmatrix} 3.4447 & 0 & -3.4447 & 0 \\ 0 & 1.9822 & 0 & -1.9822 \end{bmatrix}$$

$$D_2 = \begin{bmatrix} 0.0310 & 0.0621 \\ -0.0250 & 0.1222 \end{bmatrix} \tag{42}$$

Based on the preliminarily designed PID controller, a further tuning process with respect to the plant (40) is necessary to guarantee satisfactory performance. Following the proposed methodology, the PID tuning problem has been converted to that of LQR design. Formulating the plant (40) and controller (42) into a cascaded system as (7), the optimal controller $u_1(t)$ in (8) can be obtained through the afore-mentioned method shown in Section 3, by choosing $Q = \mathrm{diag}\{1,\ 100,\ 1,\ 1,\ 2,\ 10,\ 1,\ 1,\ 0.2,\ 0.1\}$, $R = I$, as:

$$u_1(t) = -K_1 x_1(t) - K_2 x_2(t) - D_2 u_2(t) \tag{43a}$$

where

$$K_1 = \begin{bmatrix} -1.1196 & 1.8037 & 2.3540 & -4.6493 & 1.5795 & 4.0912 \\ 0.3253 & 1.0764 & 3.1699 & 4.0756 & 1.9950 & -2.8120 \end{bmatrix}$$

$$K_2 = \begin{bmatrix} -0.7877 & -0.6160 & -0.0580 & -0.0157 \\ 0.6160 & -0.7877 & 0.0445 & -0.0193 \end{bmatrix}$$

$$D_2 = \begin{bmatrix} 0.0310 & 0.0621 \\ -0.0250 & 0.1222 \end{bmatrix}$$

This indicates the tuned PID controller (A_2, B_2, K_2, D_2) has the form of:

$$\begin{aligned} G_2(s) &= D_2 + K_2(sI - A_2)^{-1}B_2 \\ &= \begin{bmatrix} -0.1688 + \frac{-0.7877}{s} + \frac{0.1998s}{s+0.2903} & 0.0310 + \frac{-0.6160}{s} + \frac{0.0311s}{s+0.5045} \\ 0.1283 + \frac{0.6160}{s} + \frac{-0.1533s}{s+0.2903} & 0.0839 + \frac{-0.7877}{s} + \frac{0.0383s}{s+0.5045} \end{bmatrix} \end{aligned} \tag{43b}$$

The eigenvalues of the optimally designed closed-loop system (16a) are:

$$\left\{ \begin{matrix} -11.2347, & -10.0564, & -2.7758, & -1.5596 \pm 1.0223i, \\ -1.6316, & -0.2645, & -0.3386, & -0.4797, & -0.5548 \end{matrix} \right\}$$

indicating that the system is asymptotically stable. Note that this is an advantage of the proposed methodology as the closed-loop system stability is guaranteed during tuning, so that the designer is free from stability post check.

Remark 3: From the controller in (43b), it is observed that the designed centralised controller has the undesirable feature that numerical coefficients for each individual PID controller have both positive and negative signs, which is contrary to decades of tradition of having the same signs. This is probably the common feature [4, 6, 9, 10] and disadvantage of multivariable PID controller design for high-degree and/or high-dimension systems.

In the above setting, parameters in the weighting matrices Q and R are selected based on the trial-and-error method, which will be increasingly more difficult with increasing system dimension. If the designer prefers some systematic way of selecting the weighting matrices, there are some other methods available, like the regional pole assignment [24]. If we select the variable $h = 0.45$ and $R = I$ in lemma 1, where h represents the relative stability, then solve the alternative Riccati equation (14), such that the optimal controller $u_1(t)$ in (8) is obtained as:

$$u_1(t) = -K_1 x_1(t) - K_2 x_2(t) - D_2 u_2(t) \tag{44}$$

where

$$K_1 = \begin{bmatrix} -0.3692 & 0.0078 & 2.1573 & -2.1740 & 1.6054 & 0.6904 \\ -0.0950 & -1.1860 & 2.7349 & 0.5702 & 2.0903 & -2.0042 \end{bmatrix}$$

$$K_2 = \begin{bmatrix} -0.1382 & -0.2673 & 0.0021 & 0.0000 \\ 0.1702 & -0.3042 & -0.0694 & 0.0000 \end{bmatrix}$$

$$D_2 = \begin{bmatrix} 0.0310 & 0.0621 \\ -0.0250 & 0.1222 \end{bmatrix}$$

The eigenvalues of the optimally designed closed-loop system (16a) are:

$$\begin{Bmatrix} -10.5804 & -6.1092 & -0.6097 & -0.5132 & -0.5545 \\ -0.5045 & -0.9000 & -0.9000 & -0.9000 & -0.9000 \end{Bmatrix},$$

from which we find that all the closed-loop eigenvalues lie to the left of the $-h$ vertical line in the complex s-plane.

In Fig. 9, the set-point responses with different PID settings are shown. Unit set-point changes were introduced in $y_1(t)$ (at $t = 0$) and $y_2(t)$ (at $t = 20$ h), and all the system states are supposed to be measurable. The proposed system with PID setting 1, has its PID parameters obtained through solving the Riccati equation (12b), in which weighting matrices are selected based on a trial-and-error method. The other proposed system with PID setting 2 is for PID parameters obtained through solving the alternative Riccati equation (14), in which only one variable h is needed for adjustment based on the regional pole assignment method [24]. Observe that the controller tune up is much easier in this case and the set-point response of the system with PID setting 2 is comparable with that of setting 1.

The designed system gives a satisfactory set-point performance, but is rather sensitive to load disturbances. Its performance (with PID setting 1) will be shown in Fig. 11, in which system plant states are assumed to be accessible. In practical systems, an observer is needed for both state accessibility and disturbance rejection. According to the derivation in Section 4, the additional feedback component due to the observation error caused by the load disturbance, can serve as feedforward compensation for the output disturbance. The residual disturbance after compensation generates the so-called 'equivalent disturbance', which is defined as:

$$d_{eq}(s) = [I - G_P(s)\hat{G}_o(s)] \cdot d(s) \tag{45}$$

where $G_P(s) = C_1[sI - (A_1 - B_1K_1)]^{-1}B_1$, $\hat{G}_o(s) = K_1[sI - (A_1 - J_oC_1)]^{-1}J_o$.

The 'equivalent disturbance' can be used as an index to measure the disturbance compensation. Defining a dual system as $A_{dual} = A_1^T$, $B_{dual} = C_1^T$, $C_{dual} = B_1^T$, and $Q_{dual} = C_{dual}^T \cdot W \cdot C_{dual}$, in which the weighting matrix W can be tuned to achieve a less 'equivalent disturbance' in (45). Let $W = \mathrm{diag}\{1000, 1\}$ and $R_{dual} = I$, then solving the Riccati equation:

$$P_{dual}A_{dual} + A_{dual}^T P_{dual} - P_{dual}B_{dual}R_{dual}^{-1}B_{dual}^T P_{dual} + Q_{dual} = 0 \tag{46}$$

yields the desired observer gain as

$$J_o = (R_{dual}^{-1}B_{dual}^T P_{dual})^T = \begin{bmatrix} 0 & 0 \\ 0 & 0 \\ -0.3036 & 0.6555 \\ -0.3039 & 0.6562 \\ 26.1560 & 11.9660 \\ 27.4783 & 12.6016 \end{bmatrix} \tag{47}$$

Remark 4: Despite the availability of systematic approaches [22–25] to select the respective weighting matrices in (11) for the controller design, a trial-and-error method may still be required for selecting appropriate weighting matrices in (46) for the observer design. This is because the designed observer performs the function of not only state estimation, but also disturbance rejection. Fast state estimation can be achieved by appropriately selecting the pole assignment region, so that the observed states quickly converge to the system states. However, as stated before, due to the existence of the biased load disturbance, observation errors inevitably exist. If the weighting matrices are selected properly, the observation error can just serve as a feedforward compensator for the output disturbance. So, a trial-and-error method may still be needed in finding suitable weighting matrices in (46) to find the multi-objective observer, which is used for both state estimation and disturbance rejection.

The resulting 'equivalent disturbance' and the original disturbance, or disturbances before and after compensation, are compared in Fig. 10, from which we see that considerable disturbance compensation has been achieved.

Simulation results are shown in Fig. 11, comparing different PID controller settings. Unit set-point changes were introduced in $y_1(t)$ (at $t = 0$) and $y_2(t)$ (at $t = 20$ h), with a unit step disturbance occurring at $t = 40$ h. The solid line represents the output performance of the real system (38) with the PID controller (43b) and observer (19) with observer gain (47). The dash-dot line represents the output of the nominal system (40) without an observer, in which plant states are assumed to be accessible. The best performance as cited in [20], with PID setting ($\beta = 0$, $f = 1$), is shown with the dotted line in Fig. 11. It is observed that the proposed method successfully achieves a better result, especially for disturbance rejection.

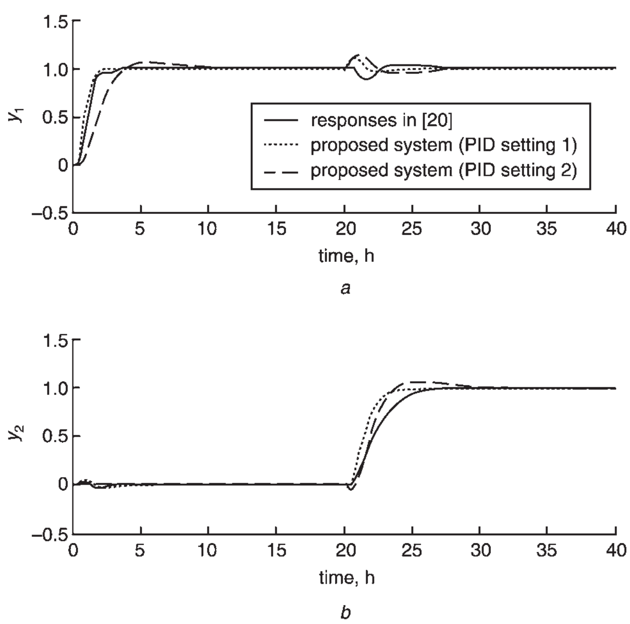

Fig. 9 *Set-point responses with different PID settings*
a y_1 as a function of time
b y_2 as a function of time

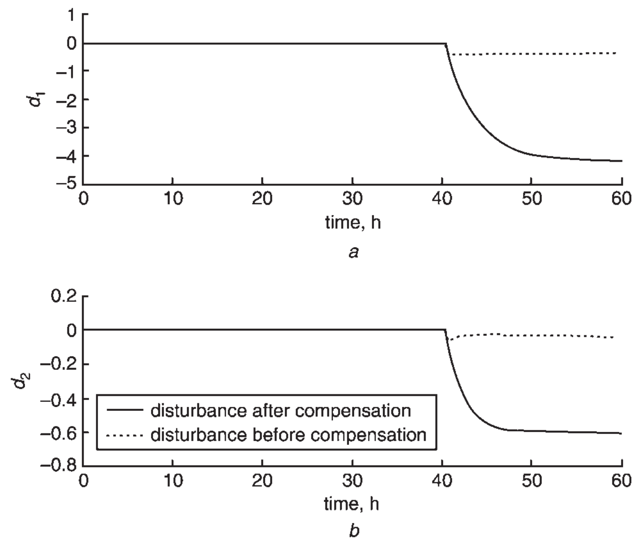

Fig. 10 *Comparison between disturbances before and after compensation*

a d_1 as a function of time
b d_2 as a function of time

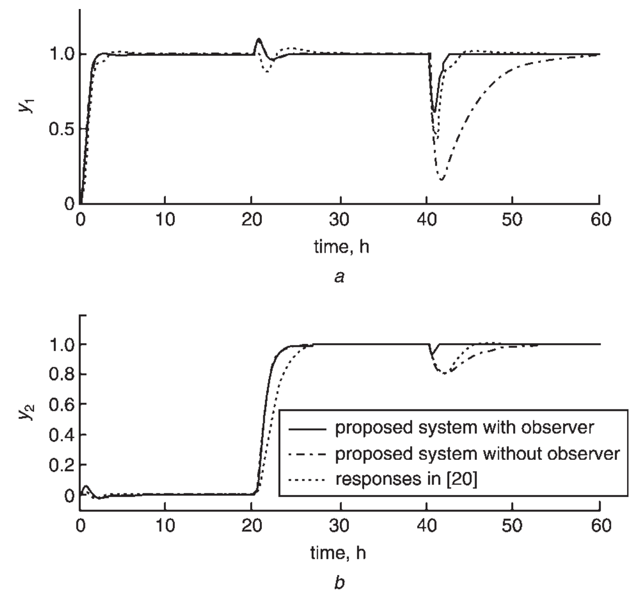

Fig. 11 *Closed-loop responses*

a y_1 as a function of time
b y_2 as a function of time

Remark 5: It is fair to point out that the method developed in [20] considered traditional decentralised PID control and did not require knowledge of the poles of the disturbed model. As a result, the proposed centralised control method performs somewhat better than the method in [20].

Next, let us investigate the sensitivity of the designed system to the disturbance poles variation. Suppose the disturbance poles are off by +25% and −25% respectively, that is the disturbance models are respectively the following:

$$\hat{d}_1(s) = \begin{bmatrix} \dfrac{-4.243e^{-0.4s}}{1.25 \times 3.445s + 1} \\ \dfrac{-0.601e^{-0.4s}}{1.25 \times 1.982s + 1} \end{bmatrix} \boldsymbol{d}(s) \qquad (48a)$$

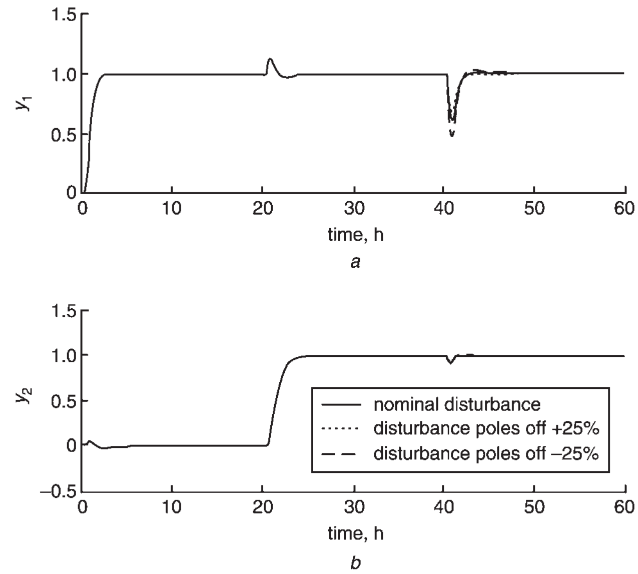

Fig. 12 *Proposed system responses in cases of disturbance poles variation*

a y_1 as a function of time
b y_2 as a function of time

$$\hat{d}_2(s) = \begin{bmatrix} \dfrac{-4.243e^{-0.4s}}{0.75 \times 3.445s + 1} \\ \dfrac{-0.601e^{-0.4s}}{0.75 \times 1.982s + 1} \end{bmatrix} \boldsymbol{d}(s) \qquad (48b)$$

Then, the same controller (43*a*) and observer gain (47) are applied to the system with the nominal disturbances in (38), and the above-mentioned disturbances $\hat{d}_1(s)$ and $\hat{d}_2(s)$ in (48), respectively.

The simulation results are shown in Fig. 12. It is observed that the proposed controller/observer still achieves robust performance for disturbance rejection in cases where the disturbance poles are off by +25% and −25% respectively.

7 Conclusions

An LQR-based design methodology has been presented to design MIMO PID controllers for multivariable analog systems with load disturbances. While the proposed method uses a more complicated MIMO PID controller, requires an observer and may have lower integrity to loss of a sensor or actuator due to failure or maintenance than the traditional controller, it offers the following notable advantages over existing traditional design methods. Firstly, the MIMO optimal PID parameters are determined by tuning the weighting matrices in the performance indices. Secondly, during tuning processes, the closed-loop system stability is guaranteed. Thirdly, there are no specific requirements on system stability, low-degree and/or low-dimension model, minimum-phase property and plant decoupling. Fourthly, the developed observer-based optimal PID controller is able to act as a set-point controller and disturbance controller for a high-degree and/or high-dimension multivariable system with unmeasurable disturbance.

The simulation results indicate that the proposed methodology is easy to implement, and provides good performance in both set-point response and disturbance rejection. Further research extending the presented methodology to the design of multivariable PID controllers for MIMO analog systems with large modelling errors caused by time delays is currently ongoing.

8 Acknowledgment

This work was supported in part by the US Army Research Office under grant 19-02-1-0321 and by NASA-JSC under grant NNJ04HF32G.

9 References

1 Zhang, Y., Wang, Q.G., and Astrom, K.J.: 'Dominant pole placement for multi-loop control systems', *Automatica*, 2002, **38**, pp. 1213–1220
2 Wang, Q.G., Hang, C.C., and Yang, X.P.: 'Single-loop controller design via IMC principles', *Automatica*, 2001, **37**, pp. 2041–2048
3 Wang, Q.G., Ru, H., and Huang, X.G.: 'An effective frequency domain approach to tuning non-PID controllers for high performance', *ISA Trans.*, 2002, **41**, pp. 37–49
4 Zheng, F., Wang, Q.G., and Lee, T.H.: 'On the design of multivariable PID controllers via LMI approach', *Automatica*, 2002, **38**, pp. 517–526
5 Koivo, H.N., and Tanttu, J.T.: 'Tuning of PID controllers: Survey of SISO and MIMO techniques'. IFAC Conf. on Intelligent Tuning and Adaptive Control, Singapore, 1991, pp. 75–80
6 Dong, J., and Brosilow, C.B.: 'Design of robust multivariable PID controllers via IMC'. Proc. American Control Conf., Albuquerque, NM, 1997, pp. 3380–3384
7 Isaksson, A., and Hgglund, T. (Eds.): 'Special Issue on PID Control'. *IEE Proc. Control Theory Appl.*, 2002, **149**, (1), pp. 1–81
8 Tan, K.K. (Ed.): 'Special Issue on Advances in PID Control', *Asian J. Control*, 2002, **4**, (4), pp. 364–508
9 Wang, Q.G., Zou, Q., Lee, T.H., and Bi, Q.: 'Autotuning of multivariable PID controllers from decentralized relay feedback', *Automatica*, 1997, **33**, pp. 319–330
10 Tan, W., Chen, T., and Marquez, H.J.: 'Robust controller design and PID tuning for multivariable processes', *Asian J. Control*, 2002, **4**, (4), pp. 439–451
11 Deshpande, P.B.: 'Multivariable process control' (Instrument Society of America, 1991)
12 Szita, G., and Sanathanan, C.K.: 'Model matching controller design for disturbance rejection', *J. Franklin Inst.*, 1996, **333**, (5), pp. 747–772
13 Goodwin, G.C., Graebe, S.F., and Salgado, M.E.: 'Control system design' (Prentice Hall, 2001)
14 Busawon, K.K., and Kabore, P.: 'Disturbance attenuation using proportional integral observers', *Int. J. Control*, 2001, **74**, (6), pp. 618–627
15 Hou, Y., Gao, Z., Jiang, F., and Boulter, B.T.: 'Active disturbance rejection control for web tension regulation'. Proc. 40th IEEE Conf. on Decision and Control, Orlando, FL, USA, December 2001, pp. 4974–4979
16 Kempf, C.J., and Kobayashi, S.: 'Disturbance observer and feedforward design for a high-speed direct-drive positioning table', *IEEE Trans. Control Syst. Technol.*, 1997, **7**, (5), pp. 513–526
17 Astrom, K.J., and Hagglund, T.: 'PID controllers: theory, design, and tuning' (Instrument Society of America, 1995)
18 Chen, C.F., and Shieh, L.S.: 'A novel approach to linear model simplification', 1968, **8**, (6), pp. 561–570
19 Hutton, M.F., and Friedland, B.: 'Routh approximations for reducing order of linear time-invariant systems', *IEEE Trans. Autom. Control*, 1995, **20**, pp. 329–337
20 Chen, D., and Seborg, D.E.: 'Multiloop PI/PID controller design based on Gershgorin bands', *IEE Proc. Control Theory Appl.*, 2002, **149**, (1), pp. 68–73
21 Ogata, K.: 'Modern control engineering' (Prentice Hall, 1996)
22 Kwakernaak, H., and Sivan, R.: 'Linear optimal control systems' (John Wiley, 1972)
23 Kawasaki, N., and Shimemura, E.: 'Determining quadratic weighting matrices to locate poles in a specified region', *Automatica*, 1983, **19**, pp. 557–560
24 Shieh, L.S., Dib, H.M., and Ganesan, S.: 'Linear quadratic regulators with eigenvalue placement in a specified region', *Automatica*, 1988, **24**, (6), pp. 819–823
25 Shieh, L.S., Liu, Z., and Sunkel, J.W.: 'Optimal uniform-damping ratio controller for sequential design of multivariable systems', *Int. J. Syst. Sci.*, 1991, **22**, (8), pp. 1371–1389
26 Zhou, K., and Doyle, J.C.: 'Essentials of robust control' (Prentice Hall, 1998), p. 227
27 Marshall, J.E.: 'Control of time-delay systems' (IEE, London, UK, 1979)
28 Wang, Q.G., Bi, Q., and Zhang, Y.: 'Partial internal model control', *IEEE Trans. Ind. Electron.*, 2001, **48**, (5), pp. 976–982
29 Morari, M., and Zafiriou, E.: 'Robust process control' (Prentice Hall, 1989)